Supporting Information for "Assessing the time of emergence of global ocean fish biomass using ensemble climate to fish simulations"

Nicolas Barrier[1] *, Olivier Maury[1], Roland Seferian[2], Yeray Santana-Falcón[2], Matthieu Lengaigne[1]

[1]MARBEC, Univ. Montpellier, CNRS, Ifremer, IRD, Sète, France

[2]CNRM (Université de Toulouse, Météo-France, CNRS)

1. Model description

In this section, the full description of the APECOSM model given in Barrier et al. 2023 is reproduced.

We use the Apex Predators Ecosystem Model (APECOSM, Maury et al., 2007; Maury, 2010) to simulate the energy transfer through marine ecosystems. APECOSM is a eulerian ecosystem model that represents the three-dimensional dynamics of size-structured pelagic populations and communities mechanistically. It integrates individual, population and community levels and includes the effects of life-history diversity with a trait-based approach (Maury & Poggiale, 2013). In APECOSM, energy uptake and utilization for individual growth, development, reproduction, somatic and maturity maintenance are modeled according to the Dynamic Energy Budget (DEB) theory (Koojman, 2010). The

*IRD, Marbec

DEB theory is a comprehensive mechanistic theory of metabolism. It has been extensively tested empirically. In APECOSM, it allows the dynamics of the main components of metabolism and life history and their size, temperature and food dependence to be represented together. In addition to metabolism, APECOSM considers important ecological processes such as opportunistic size-structured trophic interactions and competition for food, predatory, disease, ageing and starvation mortality, key physiological aspects such as vision and respiration, as well as essential processes such as three-dimensional passive transport by marine currents and active habitat-based movements (Faugeras & Maury, 2005), schooling and swarming (see Maury et al., 2007; Maury & Poggiale, 2013; Maury, 2017 for a detailed description of the model).

As discussed in Maury & Poggiale (2013), size-based predation implies that predation rates are controlled by the ratio of sizes between prey and predators (all organisms can be potentially predators and preys at the same time, depending on their relative size, cf. equation D1 of Maury & Poggiale (2013) for the detailed equation of the selectivity curve). Opportunistic predation implies that preys of a given weight are eaten in proportion to their selected available biomass relatively to the biomass of all possible preys available.

All the metabolic rates are temperature-dependent and corrected by an Arrhenius factor (Maury et al., 2007; Maury & Poggiale, 2013). While it can be prescribed in the model configuration, no preferred temperature range has been used in this study. Therefore, while temperature influences metabolism and swimming speed, its horizontal gradient does not influence the direction and magnitude of horizontal active swimming.

In APECOSM, the dynamics of communities is determined by integrating the core state equation below:

$$\partial_t \varepsilon = \underbrace{-\partial_w(\gamma\varepsilon) + \frac{\gamma}{w}\varepsilon}_{Growth} \quad \underbrace{-M\varepsilon}_{Mortalities} \quad \underbrace{-\overrightarrow{\nabla}.(\overrightarrow{V}\varepsilon)}_{3DAdv} \underbrace{+\overrightarrow{\nabla}.(D\overrightarrow{\nabla}\varepsilon)}_{3DDiff.} \tag{1}$$

where ε is the organisms' biomass density in the community, w their individual weight, γ is the growth rate, M represents the different mortality rates (computed using equation 12 of Maury & Poggiale 2013), V and D the sum of 3D passive and active velocities and diffusivity coefficients (computed following Faugeras & Maury 2005). The growth contribution is made of an advection (i.e. the biomass transfer along the size-spectrum, left-hand side) and a source term (i.e. biomass creation, right-hand side). Reproduction is considered through a Dirichlet boundary condition that injects the reproductive outputs from all mature organisms in w_0.

In APECOSM, the energy ingested by organisms fuels individual metabolism according to the DEB theory. Ingestion is proportional to a functional Holing type II response function that depends on the size-dependent visibility of prey, their aggregation in schools and temperature. This functional response can be written in a simplified way as follows:

$$f_w = \frac{P_w}{C_w + P_w} \tag{2}$$

with P_w the prey biomass that is available to predator of size w and C_w the half-saturation constant.

In the APECOSM model, oxygen concentration only modifies the horizontal and vertical habitat of the different communities and size-classes and do not modify, in its current state, the biological parameters or the physiological rates. Considering the region of interest of

the given study, this limitation has barely no consequence. Which would not be the case if analysing outputs within an Oxygen Minimum Zone (OMZ).

The APECOSM simulations used in this study are forced by three-dimensional temperature, horizontal current velocities, dissolved oxygen concentration, diatoms, mesozooplankton, microzooplankton and big particulate organic matter carbon concentrations (Aumont et al., 2015) and solar radiation outputs from the IPSL-CM6-LR simulations. Solar radiation are converted into Photosynthetic Active Radiation (PAR) using a constant coefficient of 0.43. Nutrients concentrations are not used as a forcing to Apecosm. The IPSL-CM6-LR simulations used in this study are deployed on the tripolar ORCA1 grid (Madec & Imbard, 1996), with a 1° nominal horizontal resolution and a refined 1/3° meridional resolution in the equatorial band. The vertical resolution ranges from 1m at the surface to 100m at 1 kilometer depth and varies over time, following Levier et al. (2007).

The APECOSM simulations run with a daily time step for the biological processes, which is decomposed into a day/night cycle, the duration of which depends on latitude and day of the year (Forsythe et al., 1995). A sub time-stepping ($dt = 0.8h$) is used for horizontal advection and diffusion to ensure numerical stability.

The depth dimension is explicit, i.e. each biological variable (mortality, functional response) is computed in 3 dimensions (depth, latitude, longitude). The vertical distribution is thus determined from habitat functions that depend on the choice of the communities. In this study, three interactive communities are simulated:

- The epipelagic community, which includes the organisms that are feeding during the day near the surface such as yellowfin or skipjack tunas for example. Its vertical

distribution is influenced by light and visible food during daytime as well as temperature and oxygen during both day and night, while its functional response is influenced by light and temperature.

• The migratory mesopelagic community, which feeds in the surface layer at night and migrates to deeper waters during the day. Its vertical distribution is influenced by light and visible food during the night.

• The resident mesopelagic community, which remains at depth during both night and day. Its vertical distribution is influenced by light and visible food during the day.

To ensure that the size-spectrum is fully unfolded and a pseudo-steady state is achieved, the model was integrated successively over three 1958-2018 cycles. It was first initialized with an arbitrary small biomass value in each size-class and community and integrated from 1958 to 2018 (61 years). Then, the end of this first integration phase was used to run another cycle, which in turn was used to initialize the simulation analyzed in this study.

For each community, equation 1 is integrated over 100 logarithmically distributed size classes, ranging from $0.123cm$ to $196cm$. Since saving the outputs in 3D for the 3 communities and 100 size-classes is very costly, mortality rate, growth rate and functional response for each community and size are vertically averaged as follows:

$$F(y,x,c,w) = \frac{\sum_{z=0}^{H} F(z,y,x,c,w)B(z,y,x,c,w)}{\sum_{z=0}^{H} B(z,y,x,c,w)} \tag{3}$$

with x the longitude, y the latitude, z the depth, c the community, w the size-class, F the variable to consider (functional response, mortality rate, growth rate) and B the 3D biomass (in $J.m^{-3}$).

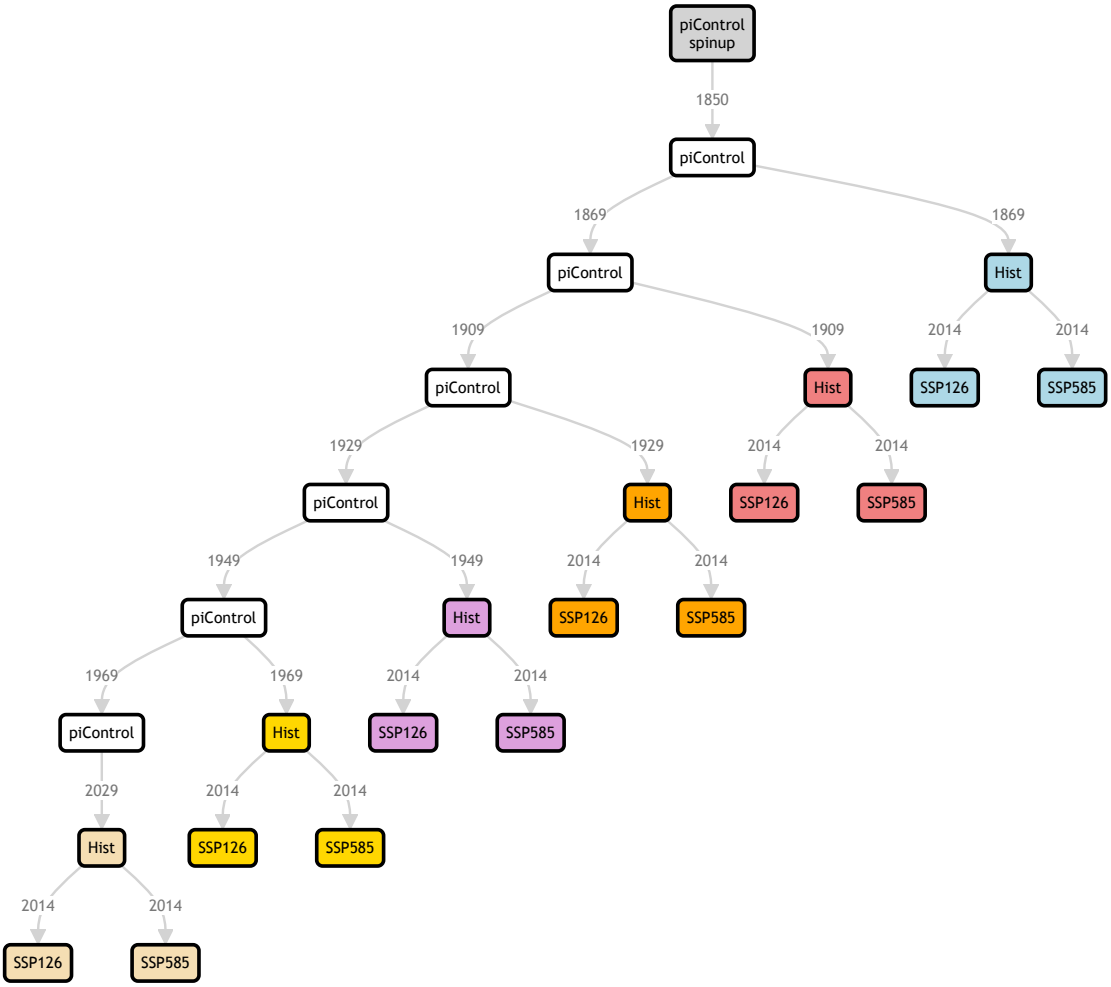

Figure S1. Schematic of the simulation protocol. The years correspond to the restart year used to integrate the following simulation.

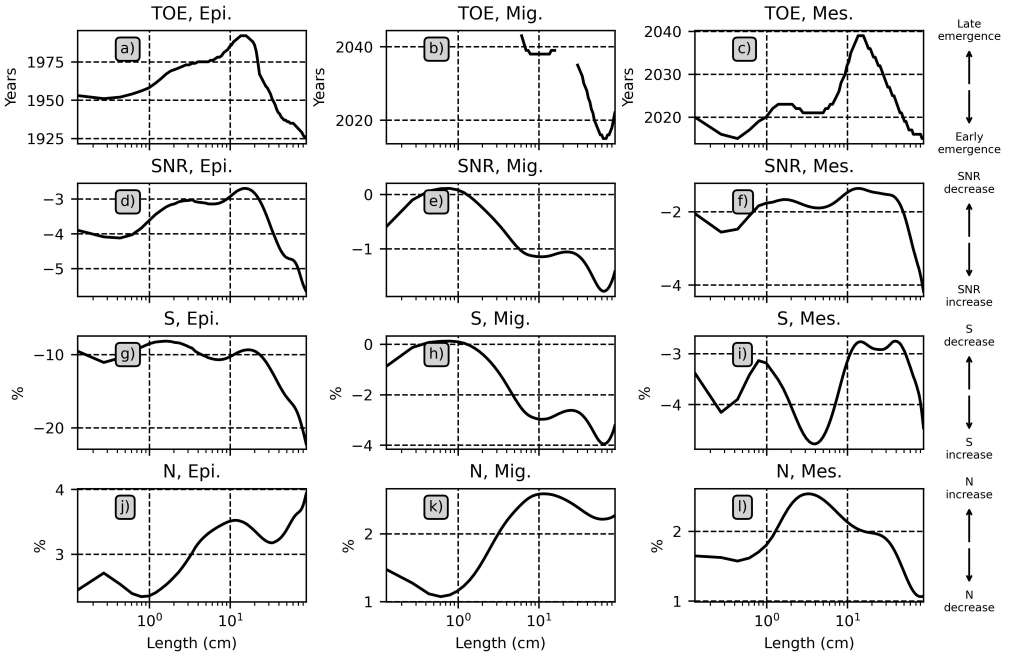

Figure S2. Time of emergence (a-c), signal to noise (d-f) ratio, relative signal (g-i) and relative noise (j-l) for epipelagic (left), migratory (middle) and mesopelagic (right) communities for the SSP1-2.6 scenario. The y-axis are ordered in a way to facilitate the interpretation of the results.

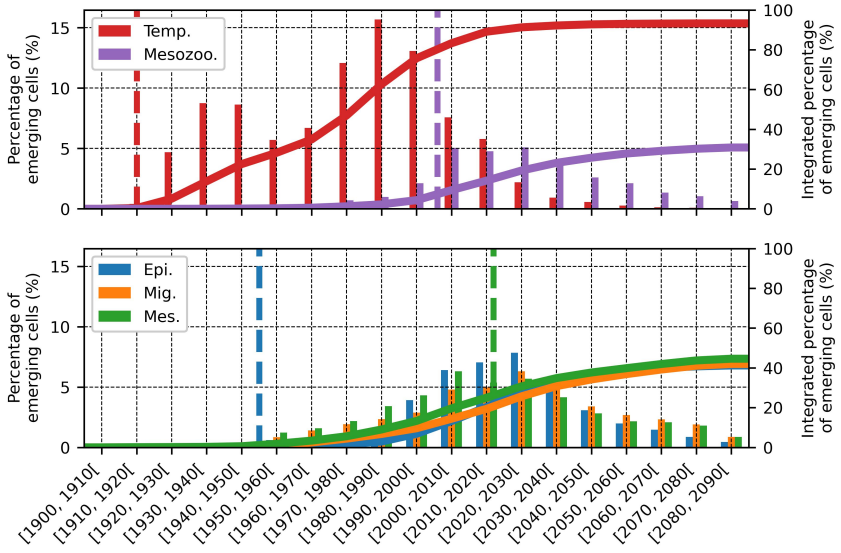

Figure S3. Percentage of the ocean surface where a signal has emerged at grid scale during a given decade (x-axis) for SST (red bars) mesozooplankton concentration at the surface (purple bars), biomass of the epipelagic fish community (blue), mesopelagic migratory fish community (orange), mesopelagic resident fish community (green) in the SSP1-2.6 scenario. The continuous lines show the corresponding cumulative percentages. The dashed vertical lines indicate the ToE of global mean time-series.

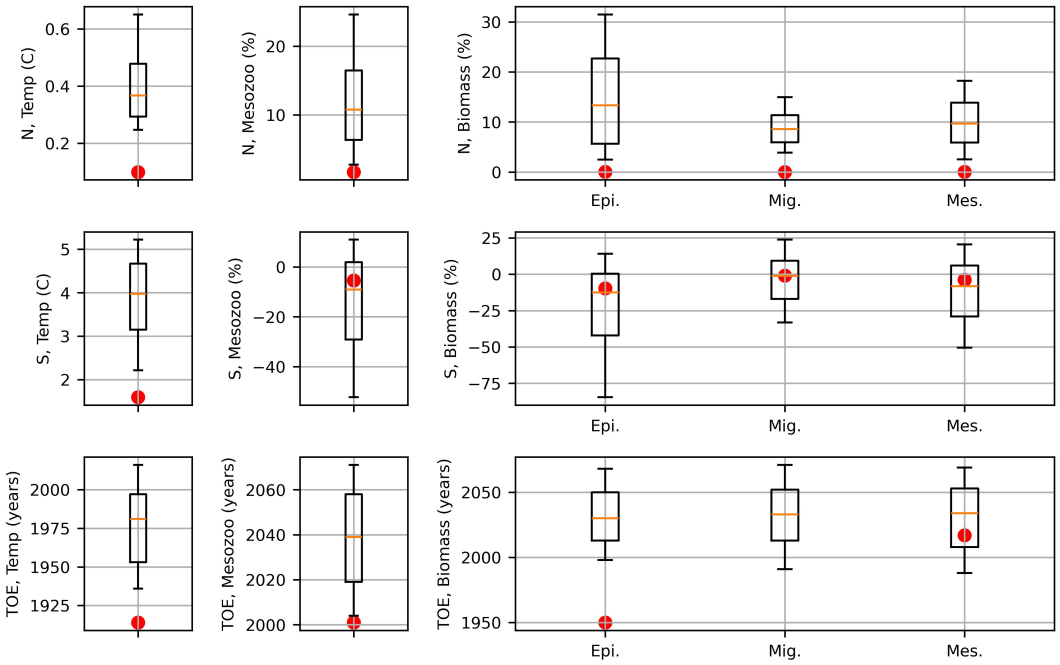

Figure S4. Whisker plot showing the 10^{th}, 25^{th}, 50^{th}, 75^{th} and 90^{th} percentiles of spatial noise N, signal S and ToE for sea surface temperature, surface mesozooplankton and fish biomass in the SSP1-2.6 scenario. Red dots indicate the values obtained from the global time series. Mesozooplankton and fish biomass noise and signal are represented in anomalies relative to the historical (1850-1950) global mean value.

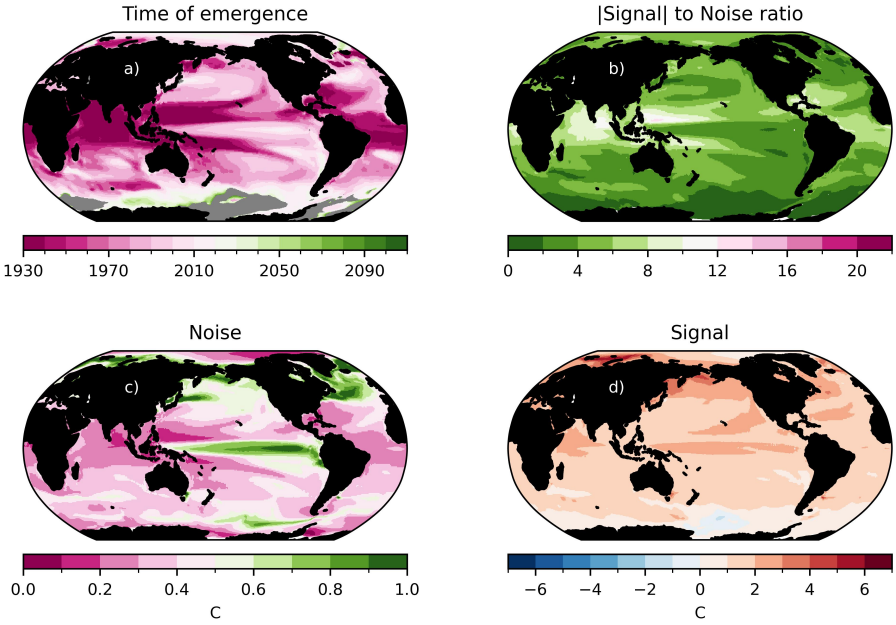

Figure S5. Maps of ToE (a), SNR (b), noise (c) and signal (d) for SST. Noise is calculated as the standard deviation of the anomalies relative to the climate change signal. Signal is calculated as the difference between the SSP1-2.6 temperature averaged over the 2070-2100 period and the historical temperature averaged between 1850 and 1900. In a), grey shadings indicate areas that have not emerged.

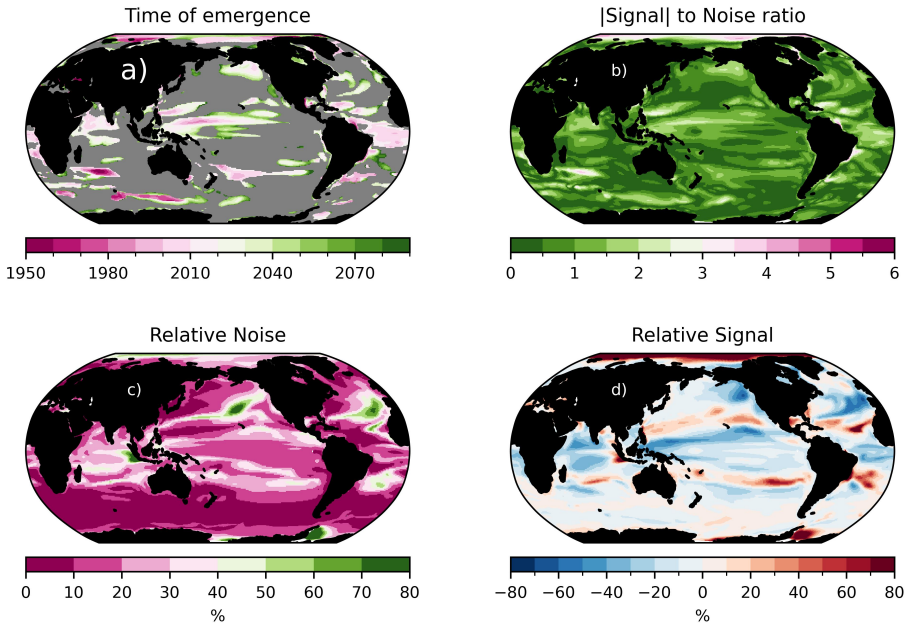

Figure S6. Time of emergence (a), signal-to-noise ratio (b), noise (c) and signal (d) for sea surface mesozooplankton concentration in the SSP1-2.6 scenario. The noise is given as the standard deviation of the anomalies relative to the climate change signal. The signal is provided as the difference between the SSP1-2.6 mesozooplankton averaged over the 2070-2100 period and the historical mesozooplankton averaged between 1850 and 1900. The latter is also used to normalise the standard deviation and signal, which are presented as percentages. In a), grey shading indicates areas that have not emerged.

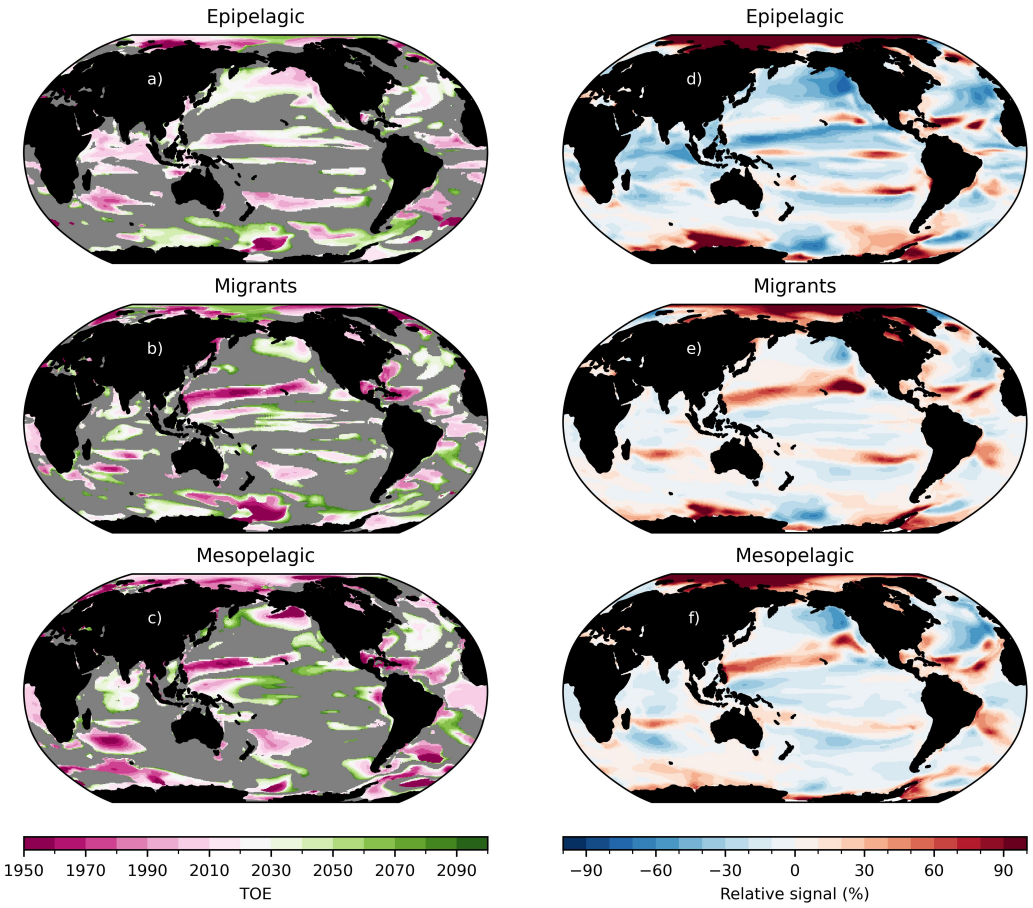

Figure S7. (a-b-c) ToE maps of fish biomass in the SSP1-2.6 scenario for each community, with non-emerging areas in grey. (d-e-f) Relative climate change signal for each of the three communities, computed as the multi-member mean difference between the SSP5-8.5 fish biomass averaged over the 2070-2100 period and the historical biomass averaged between 1850 and 1900. The latter is also used to normalise the signal and represent it as a percentage.

References

Aumont, O., Ethé, C., Tagliabue, A., Bopp, L., & Gehlen, M. (2015, August). PISCES-v2: An ocean biogeochemical model for carbon and ecosystem studies. *Geoscientific Model Development*, *8*(8), 2465–2513. doi: 10.5194/gmd-8-2465-2015

Barrier, N., Lengaigne, M., Rault, J., Person, R., Ethé, C., Aumont, O., & Maury, O. (2023, April). Mechanisms underlying the epipelagic ecosystem response to ENSO in the equatorial Pacific ocean. *Progress in Oceanography*, *213*, 103002. doi: 10.1016/j.pocean.2023.103002

Faugeras, B., & Maury, O. (2005). An advection-diffusion-reaction size-structured fish population dynamics model combined with a statistical parameter estimation procedure: Application to the Indian Ocean skipjack tuna fishery. *Mathematical Biosciences and Engineering*, *2*(4), 719. doi: 10.3934/mbe.2005.2.719

Forsythe, W. C., Rykiel, E. J., Stahl, R. S., Wu, H.-i., & Schoolfield, R. M. (1995, June). A model comparison for daylength as a function of latitude and day of year. *Ecological Modelling*, *80*(1), 87–95. doi: 10.1016/0304-3800(94)00034-F

Koojman, S. (2010). *Dynamic Energy Budget theory for metabolic organisation* (Third ed.).

Levier, B., Tréguier, A.-M., Madec, G., & Garnier, V. (2007). *Free surface and variable volume in the NEMO code.*

Madec, G., & Imbard, M. (1996, May). A global ocean mesh to overcome the North Pole singularity. *Climate Dynamics*, *12*(6), 381–388. doi: 10.1007/BF00211684

Maury, O. (2010, January). An overview of APECOSM, a spatialized mass balanced "Apex Predators ECOSystem Model" to study physiologically structured tuna population dynamics in their ecosystem. *Progress in Oceanography*, *84*(1), 113–117. doi: 10.1016/j.pocean.2009.09.013

Maury, O. (2017, August). Can schooling regulate marine populations and ecosystems? *Progress*

in Oceanography, *156*(Supplement C), 91–103. doi: 10.1016/j.pocean.2017.06.003

Maury, O., & Poggiale, J.-C. (2013, May). From individuals to populations to communities: A dynamic energy budget model of marine ecosystem size-spectrum including life history diversity. *Journal of Theoretical Biology*, *324*, 52–71. doi: 10.1016/j.jtbi.2013.01.018

Maury, O., Shin, Y.-J., Faugeras, B., Ben Ari, T., & Marsac, F. (2007, September). Modeling environmental effects on the size-structured energy flow through marine ecosystems. Part 2: Simulations. *Progress in Oceanography*, *74*(4), 500–514. doi: 10.1016/j.pocean.2007.05.001